0888-8809/08/$15.00/0
Printed in U.S.A.

Molecular Endocrinology 22(5):1200–1212

doi: 10.1210/me.2007-0485

Adipose Triglyceride Lipase Regulation of Skeletal Muscle Lipid Metabolism and Insulin Responsiveness

Matthew J. Watt, Bryce J. W. van Denderen, Laura A. Castelli, Clinton R. Bruce, Andrew J. Hoy, Edward W. Kraegen, Lance Macaulay, and Bruce E. Kemp

St. Vincent's Institute of Medical Research and Department of Medicine (M.J.W., B.J.W.v.D., B.E.K.), University of Melbourne, Fitzroy, Victoria 3065, Australia; Commonwealth Scientific and Industrial Research Organization Molecular and Health Technologies (L.A.C., L.M., B.E.K.), Parkville, Victoria 3052, Australia; Cellular and Molecular Metabolism Laboratory (C.R.B.), Baker Heart Research Institute, Prahran, Victoria 8008, Australia; and Diabetes and Obesity Research Program (C.R.B., A.J.H., E.W.K.), Garvan Institute of Medical Research, Darlinghurst, New South Wales 2010, Australia

Adipose triglyceride lipase (ATGL) is important for triglyceride (TG) metabolism in adipose tissue, and ATGL-null mice show increased adiposity. Given the apparent importance of ATGL in TG metabolism and the association of lipid deposition with insulin resistance, we examined the role of ATGL in regulating skeletal muscle lipid metabolism and insulin-stimulated glucose disposal. ATGL expression in myotubes was reduced by small interfering RNA and increased with a retrovirus encoding GFP-HA-ATGL. ATGL was also overexpressed in rats by *in vivo* electrotransfer. ATGL was downregulated in skeletal muscle of obese, insulin-resistant mice and negatively correlated with intramyocellular TG levels. ATGL small interfering RNA in myotubes reduced TG hydrolase activity and increased TG content, whereas ATGL overexpression induced the reciprocal response, indicating that ATGL is an essential TG lipase in skeletal muscle. ATGL overexpression in myotubes increased the oxidation of fatty acid liberated from TG and diglyceride and ceramide contents. These responses in cells were largely recapitulated in rats overexpressing ATGL. When ATGL protein expression and TG hydrolase activity in obese, insulin-resistant rats were restored to levels observed in lean rats, TG content was reduced; however, the insulin resistance induced by the high-fat diet persisted. In conclusion, ATGL TG hydrolysis in skeletal muscle is a critical determinant of lipid metabolism and storage. Although ATGL content and TG hydrolase activity are decreased in obese, insulin-resistant phenotypes, overexpression does not rescue the condition, indicating reduced ATGL is unlikely to be a primary cause of obesity-associated insulin resistance. (*Molecular Endocrinology* 22: 1200–1212, 2008)

SKELETAL MUSCLE CONTAINS significant triglyceride (TG) stores that are a source of fatty acids (FAs) for energy metabolism (1) and various cell functions including the generation of second messengers in signaling cascades, *e.g.* ceramides, apoptosis, and cellular differentiation. TG accumulates in the muscle of obese individuals and type 2 diabetes patients and positively associates with insulin resistance (2, 3). Despite the role of skeletal muscle TG in energy metabolism and its association with the development of insulin resistance, the factors regulating TG mobilization in this tissue are poorly understood.

First Published Online January 17, 2008

Abbreviations: ATGL, Adipose triglyceride lipase; DG, diglyceride; FA, fatty acid; GFP, green fluorescent protein; HA, hemagglutinin; HSL, hormone-sensitive lipase; IMTG, intramyocellular TG; MG, monoacylglycerol; siRNA, small interfering RNA; TA, tibialis anterior; TG, triglyceride.

***Molecular Endocrinology* is published monthly by The Endocrine Society (http://www.endo-society.org), the foremost professional society serving the endocrine community.**

Hormone-sensitive lipase (HSL) has long been regarded as the key lipolytic enzyme in skeletal muscle (4–7). HSL is an intracellular neutral lipase that catalyzes the hydrolysis of TG and diglyceride (DG) and DG to monoacylglycerol (MG). HSL activity is controlled by reversible phosphorylation at five known serine residues (8, 9), by translocation to its substrate, and possibly via association with lipid droplet-associated proteins (10). Interestingly, perilipin, which is essential for adipose tissue lipolysis, is not expressed in skeletal muscle (11), suggesting important tissue-specific differences in the control of TG metabolism. The concept that HSL is the key enzyme responsible for regulating FA mobilization is contentious. $HSL^{-/-}$ mice maintain about 90% of their TG lipase activity and accumulate DG in their skeletal muscle, suggesting that HSL is not essential for TG degradation but rather is the rate-limiting enzyme for DG catabolism (12). In lysates prepared from human skeletal muscle, immunodepletion of HSL reduces total TG lipase activity by 60% (13).

Adipose TG lipase (ATGL) was recently cloned and appears to be essential for efficient TG metabolism in adipose tissue (14–17). ATGL shares several common motifs with other known TG lipases including a GXSXG motif with an active serine at position 47, an α/β-hydrolase fold and an N-terminal patatin homology domain (14, 16). ATGL exhibits high substrate specificity for the hydrolysis of TG (14, 16), and full activation appears to require interaction with the regulator CGI-58 (18). The available evidence indicates that ATGL cleaves the first FA on TG, followed by HSL cleaving DG and MG lipase cleaving MG.

ATGL is essential for the control of normal weight because overexpression of the ATGL homolog in *Drosophila* depletes fat stores and loss of ATGL activity causes obesity (19, 20). The physiological mechanisms linking obesity to insulin resistance are complex but, at least in part, relate to defective fat metabolism resulting in the accumulation of FA metabolites, such as DG and ceramides, that inhibits insulin signaling (21). ATGL-null mice accumulate TG in several tissues and oxidize more glucose, which may result from a reciprocal decrease in FA availability and reduced uncoupled respiration (20). Significantly, ATGL-null mice displayed whole-body insulin sensitivity despite the marked accumulation of TG in important tissues for glucose metabolism, including skeletal muscle and liver. It is not possible to determine whether the metabolic alterations in ATGL-null mice resulted from reduced plasma FA delivery, secondary to decreased adipose tissue lipolysis, or were due to direct effects of ATGL in nonadipose tissues. Furthermore, the tissue-specific effects of ATGL have not been evaluated.

Skeletal muscle is quantitatively the most important site for FA uptake and oxidation and insulin-stimulated glucose disposal (22, 23), and ATGL is expressed in skeletal muscle at levels equivalent to those reported in some white adipose tissue depots (17). Previous experiments have demonstrated an important role for ATGL in adipocyte biology (20); however, its importance in the control of substrate metabolism and the pathogenesis of insulin resistance in the setting of obesity has not been evaluated. The objective of this study was to directly examine the impact of ATGL on skeletal muscle FA metabolism and insulin responsiveness.

RESULTS

ATGL Expression Is Reduced in Skeletal Muscle of Obese, Insulin-Resistant Rodents

Body mass (low fat, 31.3 ± 0.4 g; high fat, 33.9 ± 1.1 g), adiposity (epididymal fat: low fat, 234 ± 50 mg; high fat, 602 ± 117 mg), and plasma insulin (low fat, 0.30 ± 0.07 nmol/liter *vs.* high fat, 0.82 ± 0.09 nmol/liter) were increased by high-fat feeding in C57BL/6J mice. Intramyocellular TG (IMTG) was increased (Fig. 1A), and ATGL protein expression was reduced in high-fat compared with low-fat mice (Fig. 1B). IMTG was negatively associated with ATGL protein expression ($r^2 = 0.901$, Fig. 1C). HSL protein expression was reduced in high *vs.* low fat (Fig. 1F), and CGI-58 protein expression was not different between groups (data not shown). The *ob/ob* mouse was obese (epididymal fat: ob/+, 180 ± 15 mg; *ob/ob*, 852 ± 56 mg) and hyperinsulinemic (ob/+, 0.45 ± 0.14 nmol/liter; *ob/ob*, 2.82 ± 0.47 nmol/liter). IMTG was increased (Fig. 1D) and ATGL protein expression was reduced in *ob/ob* mice compared with controls (Fig. 1E). HSL protein expression was reduced in *ob/ob vs.* controls (Fig. 1F), and CGI-58 protein expression was not different between groups (data not shown). Interestingly, ATGL mRNA expression was elevated in the skeletal muscle of high-fat mice (low fat, 1.00 ± 0.13 arbitrary units; high fat, 1.62 ± 0.14 arbitrary units) and *ob/ob* mice (ob/+, 1.00 ± 0.07 arbitrary units; *ob/ob*, 2.36 ± 0.65 arbitrary units) compared with control littermates. This is consistent with our recent observation of increased ATGL mRNA yet decreased protein in the adipose tissue of obese, insulin-resistant humans (24). Together, these data demonstrate that increased IMTG found in the skeletal muscle of obese, insulin-resistant mice is associated with decreased ATGL protein expression.

ATGL Knockdown Decreases TG Lipolysis in Myotubes

There were no obvious morphological differences with transient knockdown of ATGL with small interfering RNA (siRNA). ATGL siRNA reduced ATGL protein expression by 23% (Fig. 2A) and had no effect on CGI-58 (Fig. 2A) or HSL protein expression (Fig. 2A). Basal and stimulated TG hydrolase activity was reduced in ATGL-siRNA myotubes (Fig. 2B). [^{14}C]Palmitate incorporation into TG was increased by 27% (Fig. 2C), with no differences in DG and free FA (FFA) incorporation. TG content was increased by 18% in ATGL-siRNA myotubes (Fig. 2D). Although knockdown of ATGL protein was modest, these data are consistent with ATGL's role as a TG lipase (20).

Retroviral-Mediated ATGL Overexpression Increases TG Lipolysis and Alters FA Metabolism in Myotubes

Because ATGL protein expression is reduced and TG accumulates in the skeletal muscle of obese, insulin-resistant mice, we tested the hypothesis that increasing ATGL would enhance FA turnover in muscle. Stable transfection of C2C12 myoblasts with murine green fluorescent protein (GFP)- and hemagglutinin (HA)-tagged ATGL increased ATGL protein expression 2.8-fold (Fig. 3A, band detected at 83 kDa) and coincided with increased basal and stimulated TG hydrolase activity (Fig. 3B). Endogenous ATGL (Fig. 3A, 54

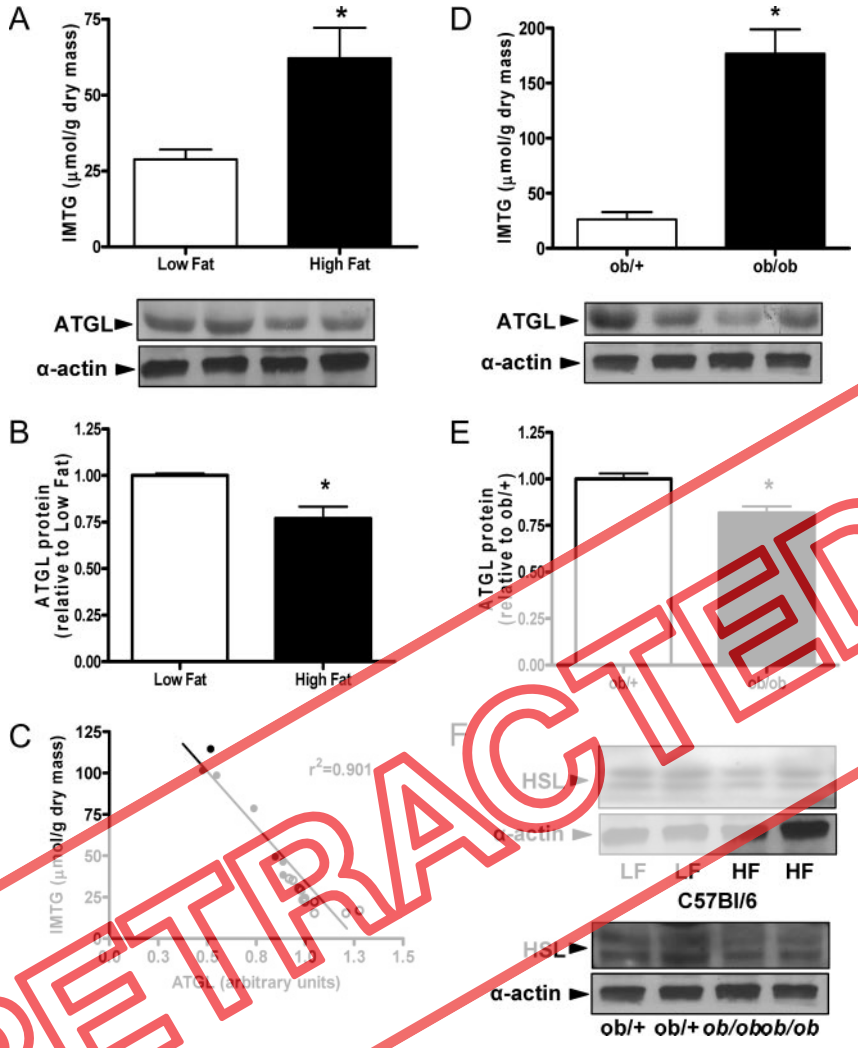

Fig. 1. ATGL Protein Expression and TG Hydrolase Activity Are Reduced in Obese, Insulin-Resistant Mice

IMTG and ATGL protein expression were determined in skeletal muscle lysates from C57BL/6J mice fed a low- or a high-fat diet (A and B) and *ob/ob* mice and heterozygous littermates (D and E). Data are presented as mean ± SEM and are expressed relative to ATGL expression in low-fat (n = 7–11) and ob/+ mice (n = 4 per group). *, $P < 0.05$. C, ATGL protein expression *vs.* IMTG content in low-fat (○) and high-fat (●) fed mice. F, HSL protein expression assessed by Western blot in skeletal muscle lysates in C57BL/6J mice fed a low-fat (LF) or a high-fat (HF) diet (*top*) and *ob/ob* mice and heterozygous littermates (*bottom*).

kDa) and HSL protein content were unaffected (data not shown) by GFP-HA-ATGL expression. Overexpression of ATGL resulted in reduced [^{14}C]palmitate incorporation into TG (Fig. 3C) and increased incorporation into DG (Fig. 3D). Because saturated and unsaturated FAs differ with respect to their propensity for oxidation and storage (25), we repeated these experiments using [^{14}C]oleate. ATGL overexpression decreased the rate of [^{14}C]oleate incorporation into TG (Fig. 3C); however, [^{14}C]oleate incorporation into DG was not different from control myotubes (Fig. 3D). Oxidation of exogenous palmitate (*i.e.* that derived from the media palmitate) was reduced by 15% in myotubes with ATGL overexpression (Fig. 3E). Total uptake of exogenous FAs was not different between GFP and ATGL (data not shown).

CGI-58 is a member of the lipase subfamily characterized by the presence of an α/β-hydrolase fold. CGI-58 interacts with ATGL and is essential for maximal ATGL enzyme activity (18). Mutations in the human *CGI-58* gene causes Chanarin-Dorfman syndrome that results in neutral lipid accumulation in several tissues including skeletal muscle (26). CGI-58 overexpression alone had no effect on TG hydrolase activity or any other aspect of fat metabolism assessed (data not shown). Overexpression of ATGL (2.9-fold) and CGI-58 (2.8-fold) (Fig. 3A, 40 kDa) did not affect endogenous ATGL and CGI-58 protein (Fig. 3A, 54 kDa and 39 kDa respectively). The double overexpression increased TG hydrolase activity above ATGL alone (Fig. 3B). The incorporation of FAs into TG was decreased for palmitate and oleate treatment,

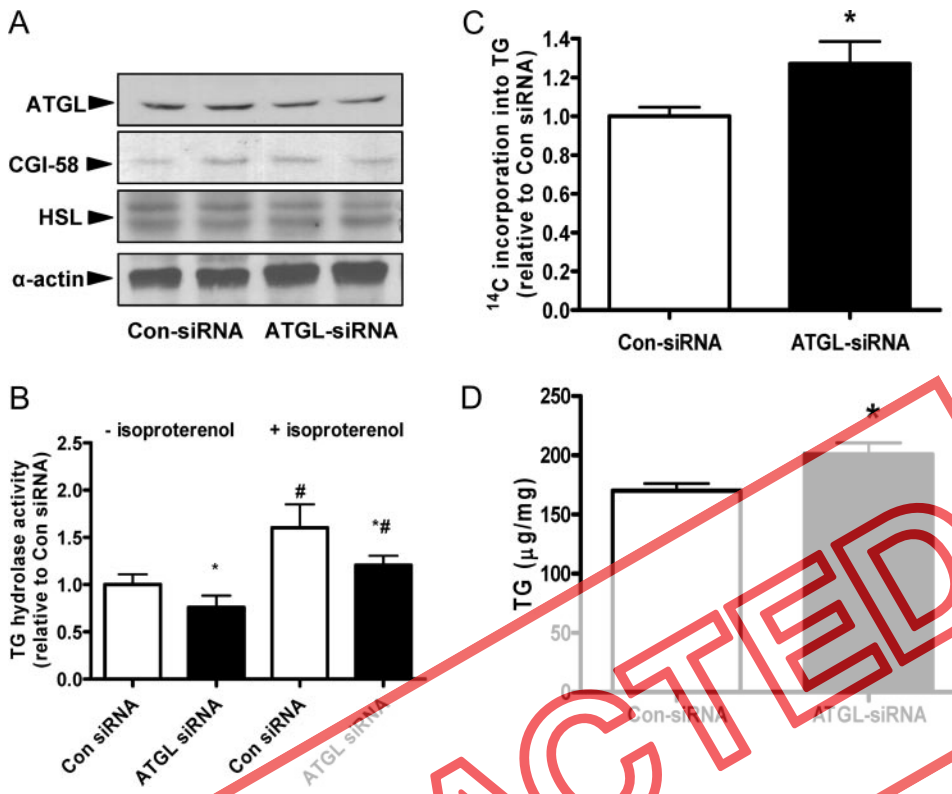

Fig. 2. Transient Knockdown of ATGL in C2C12 Myotubes

siRNA-mediated knockdown in C2C12 myotubes was achieved by liposomal transfection with either control siRNA (Con-siRNA) or ATGL-specific siRNA (ATGL-siRNA) at d 4 of differentiation (four experiments, n = 3 per group per experiment). A, ATGL and CGI-58 protein expression; B, TG hydrolase activity (Con siRNA, 1.47 ± 0.03 nmol/h·mg protein); C, [^{14}C]palmitate incorporation into TG (Con siRNA, 13.3 ± 0.6 nmol/h·mg protein); D, TG content were determined at d 5 of differentiation. Data are mean ± SEM. *, $P < 0.05$ *vs.* Con-siRNA; #, $P < 0.05$, with isoproterenol *vs.* without isoproterenol for the same treatment.

respectively (Fig. 3C), and DG esterification was increased with exposure to palmitate but not oleate (Fig. 3D). The oxidation of exogenous FAs was decreased by 21% (Fig. 3E). We next determined whether the increase in TG hydrolase activity resulted in enhanced oxidation of endogenous FAs. Cells were pulsed with 0.5 mM [^{14}C]oleate for 24 h to prelabel the intracellular lipid pools. These experiments were not performed with palmitate because significant apoptosis occurs (27). Endogenous FA oxidation (oleate derived from predominantly TG) was increased by 49 and 127% for ATGL and ATGL/CGI-58, respectively (Fig. 3F). These calculations assume that all of the endogenous FAs oxidized were derived from TG. Given that exogenous FA uptake was not different, these data indicate that ATGL overexpression increases total FA flux in myotubes. Finally, we were unable to detect the release of FAs into the culture media indicating that nonesterified FAs generated by ATGL must either be reesterified or oxidized within the myocyte.

Retroviral-Mediated ATGL Overexpression Increases Lipid Metabolites in Myotubes

DG content was increased in ATGL and ATGL/CGI-58-overexpressing cells without FA treatment (Fig. 4A). Palmitate increased DG accumulation in control cells; however, palmitate did not increase DG levels above basal levels with ATGL and ATGL/CGI-58 overexpression. The accumulation of DG is consistent with the premise that ATGL exhibits substrate specificity for TG (16). These data also indicate that HSL is insufficient to increase DG degradation to match the increased rate of TG hydrolysis. Interestingly, ceramide content was increased in ATGL-overexpressing cells, but were not different from control when ATGL and CGI-58 were concomitantly increased (Fig. 4B). Ceramide content was increased in all cell lines with exposure to palmitate and remained elevated in ATGL-overexpressing myotubes.

Retroviral-Mediated ATGL Overexpression Causes Insulin Resistance

Basal glycogen content (GFP, 6.47 ± 0.24 μg/mg protein; ATGL, 7.17 ± 0.45 μg/mg protein), basal glycogen synthesis (Fig. 5A), and basal Akt Ser473 phosphorylation (data not shown) were unaffected by ATGL overexpression whereas palmitate exposure reduced basal glycogen synthesis (Fig. 5A) and Akt Ser473 phosphorylation equally in both cell lines (data not shown). We determined insulin sensitivity in C2C12

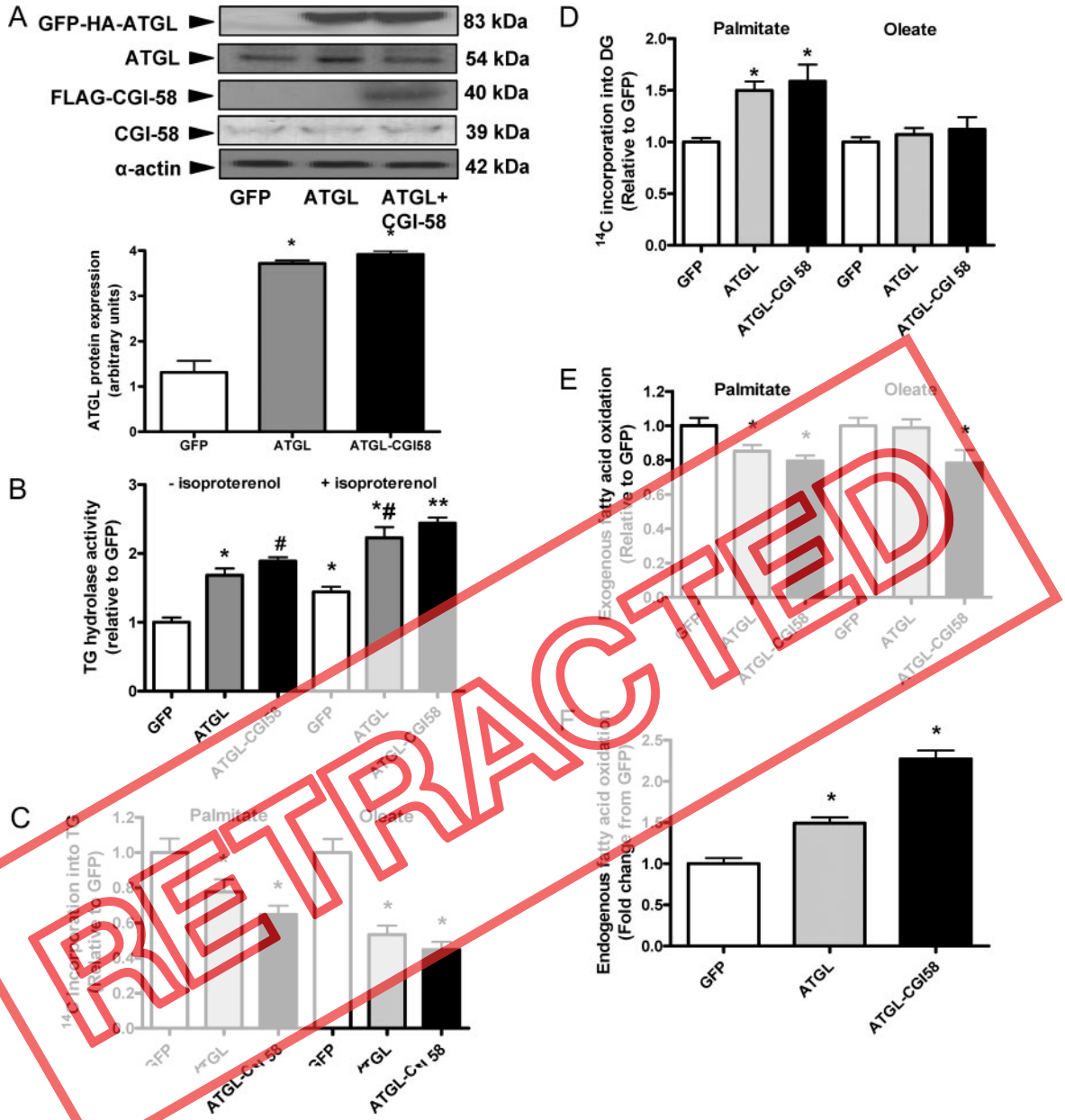

Fig. 3. Retrovirus-Mediated Overexpression of GFP-HA-ATGL and FLAG-CGI-58 in C2C12 Myotubes

Overexpression of GFP-HA-ATGL or GFP-HA (control) and FLAG-CGI58 was achieved after retrovirus-mediated infection of myoblasts as described in the *Materials and Methods*. A, Expression of native and tagged ATGL (using anti-ATGL antibody), FLAG-CGI-58 (using anti-FLAG antibody), and CGI-58 (using anti-CGI-58 antibody) were determined by Western blot. For both ATGL and CGI-58, immunoblots are presented independently because endogenous expression cannot be detected without heavily overexposing the tagged protein. The quantification in the column graph represents native plus tagged expression. B–F, TG hydrolase activity (B; GFP, 1.21 ± 0.12 nmol/h·mg protein), palmitate incorporation into TG (C; GFP, 12.6 ± 1.0 nmol/h·mg protein), DG (D; GFP, 6.6 ± 2.6 nmol/h·mg protein), and exogenous (E; 1.87 ± 0.08 nmol/h·mg protein) and endogenous (F; GFP, 0.11 ± 0.01 nmol/h·mg protein·μg triglyceride) FA oxidation were determined at d 5 of differentiation (three experiments, n = 5 per group per experiment). Data are mean ± SEM. *, $P < 0.05$ *vs.* GFP; #, $P < 0.05$ *vs.* GFP and ATGL; **, $P < 0.05$ *vs.* GFP and ATGL within the same treatment and *vs.* ATGL-CGI-58 without isoproterenol.

myotubes by measuring glycogen synthesis. Insulin-stimulated glycogen synthesis was increased above basal in all groups and was lower with ATGL overexpression when compared with GFP (Fig. 5B). Although palmitate suppressed insulin-stimulated glycogen synthesis equally in both groups, insulin-stimulated glycogen synthesis was decreased in ATGL-overexpressing cells compared with controls (Fig. 5B). Phosphorylation of Akt at Ser473 mirrored these responses (Fig. 5C).

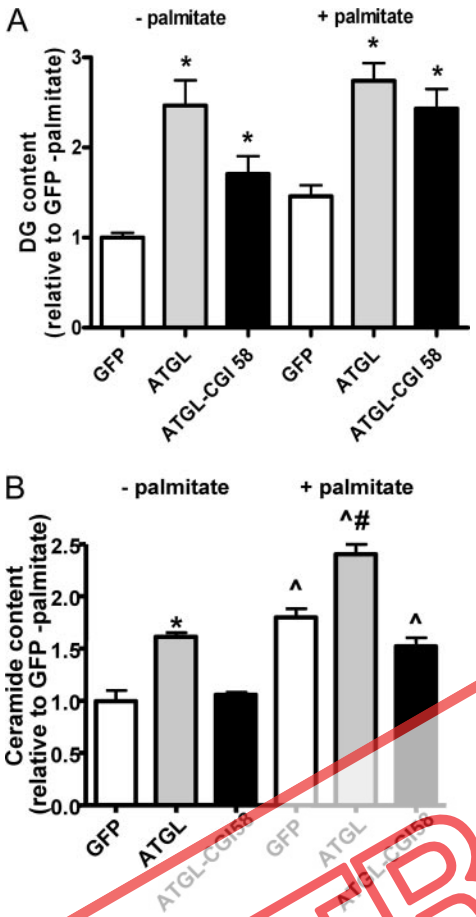

Fig. 4. Diglyceride and Ceramide Content in Myotubes Expressing GFP-HA-ATGL

DG (A) and ceramide (B) were determined by enzymatic radiometric methods in lysates from C2C12 cells expressing GFP-HA (control), GFP-HA-ATGL (ATGL), or ATGL and full-length FLAG-CGI-58 (ATGL-CGI 58) (n = 9 per group). Data are mean ± SEM. *, $P < 0.05$ *vs.* GFP without palmitate within same treatment; #, $P < 0.05$ *vs.* same cell line without palmitate; ^, $P < 0.05$ *vs.* ATGL-CGI 58 within same treatment.

Acute ATGL Overexpression Results in Lipid Metabolite Accumulation But Not Insulin Resistance in Rat Skeletal Muscle *in Vivo*

To investigate the physiological consequence of ATGL overexpression *in vivo*, we assessed lipid metabolism in rats fed a low-fat chow diet. ATGL electroporation increased ATGL protein by 25% (Fig. 6B) and did not affect HSL protein expression (Fig. 6A). ATGL expression was increased in the experimental leg of all rats. TG hydrolase activity was increased by 29% with ATGL overexpression (Fig. 6C), which resulted in a 47% reduction in muscle TG (Fig. 6D). DG and ceramide content were elevated by ATGL overexpression (Fig. 6, E and F). We performed hyperinsulinemic-euglycemic clamps to examine the insulin sensitivity of glucose metabolism in rats. During a continuous infusion of insulin at 0.25 U/kg·h, the glucose infusion rate required to maintain blood glucose at 5 mM was 36 mg/kg·min (Fig. 7A). Insulin-stimulated glucose uptake into the tibialis anterior (TA) was not different between legs (Fig. 7B), nor was the rate of insulin-stimulated glucose incorporation into glycogen (Fig. 7C).

We next evaluated whether the effects of ATGL overexpression on fat metabolism would be maintained in obesity. The high-fat diet increased fat pad mass and induced a mild hyperinsulinemia (Table 1), whereas fasting plasma glucose, FFA, and muscle glycogen content (control, 41.8 ± 4.6 μmol/g; ATGL, 40.1 ± 2.1 μmol/g) were not different. ATGL protein expression was decreased in the control leg of high-fat-fed rats, and electroporation increased ATGL by 41% and coincided with increased TG hydrolase activity and reduced TG content (Figs. 6, A–D). Importantly, the ATGL expression, TG hydrolase activity, and TG content after ATGL electroporation in high-fat-fed rats was normalized to values observed in control rats fed chow. High-fat feeding increased DG and ceramide content in both legs compared with chow-fed animals (Figs. 7, D and E); however, only ceramide was increased in ATGL compared with the control leg. Clamp plasma insulin was not different between groups (chow, 699 ± 42 pmol/liter; high-fat diet, 767 ± 47 pmol/liter; n = 8 per group). The glucose infusion rate in animals fed the high-fat diet was reduced by 24% during the hyperinsulinemic-euglycemic clamp compared with chow-fed animals (Fig. 7A). Glucose disposal (28%) and glucose incorporation into glycogen (36%) in the TA were reduced by high-fat feeding (Fig. 7, B and C). Insulin sensitivity was not different between legs after the high-fat diets, indicating that physiological ATGL overexpression cannot protect skeletal muscle against fat-induced insulin resistance.

DISCUSSION

Defective skeletal muscle FA metabolism that is characterized by the accumulation of IMTGs is a key feature of obesity and type 2 diabetes (21) and is positively associated with insulin resistance (2, 3). ATGL is an essential mediator of TG lipolysis and energy metabolism in cultured adipocytes and weight maintenance in mice and other lower-order organisms (14–17, 19, 20, 28, 29); however, the role of ATGL in skeletal muscle remains incompletely understood. The present study is the first to report the role of ATGL in skeletal muscle TG lipolysis and FA metabolism and the relationship with insulin sensitivity. Our studies showed that ATGL is down-regulated in obese, insulin-resistant phenotypes and is an important TG hydrolase in muscle that alters FA partitioning.

The function of ATGL has been studied in adipocytes and other cell lines. ATGL removes the first FA from TG, thereby generating a FA and DG substrate for degradation by HSL (16). Maximal ATGL enzyme activity requires activation by CGI-58 (18), although the

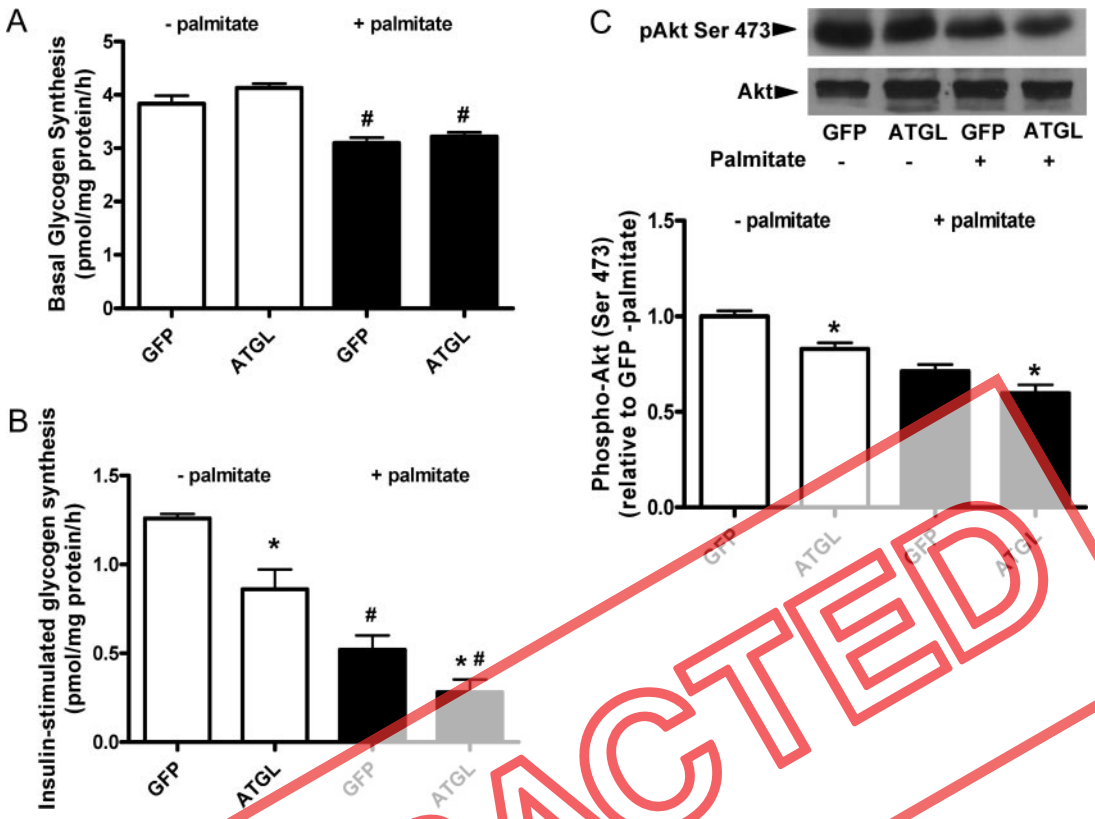

Fig. 5. Glycogen Synthesis and Akt Phosphorylation in Myotubes Stably Expressing ATGL

Retroviral-mediated overexpression of ATGL was achieved by stable transfection with a control vector (GFP) or full-length ATGL cDNA (ATGL). A, Basal glycogen synthesis in myotubes; B, insulin-stimulated glycogen synthesis was determined in myotubes and is calculated as glycogen synthesis in the presence of insulin minus glycogen synthesis in the absence of insulin (*i.e.* basal); C, insulin-stimulated Akt Ser473 phosphorylation was determined by Western blot analysis. Representative immunoblots are presented above. Basal Akt Ser473 phosphorylation (data not shown) and total Akt content were not different between treatments or cell lines. Data are mean ± SEM. *, $P < 0.05$ *vs.* GFP; #, $P < 0.05$ *vs.* without palmitate.

details of this interaction are not yet clear. ATGL appears to play a fundamental role in energy homeostasis. Overexpression of an ATGL homolog in *Drosophila* depleted fat stores, whereas loss of activity caused obesity (19). Whole-body ATGL knockout in mice resulted in supraphysiological deposition of TG, obesity, and premature death as a result of cardiac dysfunction (20). Interestingly, despite the finding of massive TG deposition in insulin-sensitive tissues such as the liver and skeletal muscle, which has been repeatedly associated with insulin resistance (2, 3), ATGL knockout mice have enhanced glucose and insulin tolerance and greater tissue-specific glucose uptake in skeletal and cardiac muscle and the liver. The mechanisms underpinning this adaptive response were not investigated.

Here, we present evidence that ATGL is a TG hydrolase in skeletal muscle. TG hydrolase activity was reduced with siRNA-mediated knockdown of ATGL and coincided with elevated TG content. Conversely, gain-of-function experiments demonstrated increased TG hydrolase activity and reduced TG content in myotubes. In further support of these findings, *in vivo* overexpression of ATGL enhanced TG hydrolase activity and halved TG content. These findings support those of Haemmerle *et al.* (20) that reported decreased TG hydrolase activity and TG accumulation in the skeletal muscle of ATGL$^{-/-}$ mice.

CGI-58 is reported to be essential for efficient TG hydrolase activity and may be rate limiting for lipolysis (18). We found that CGI-58 protein expression was not down-regulated in obese, insulin-resistant rodents. CGI-58 overexpression in myotubes did not increase TG hydrolase activity, which contrasts with a previous study in COS-7 cells overexpressing CGI-58 (18). Co-overexpression of ATGL and CGI-58 modestly increased TG hydrolase activity compared with ATGL alone. The small increase in biological activity may reflect reduced dependency of ATGL for CGI-58 in skeletal muscle and/or indicate that endogenous CGI-58 expression is sufficient to stimulate ATGL activity. ATGL overexpression was not associated with detectable increases in endogenous CGI-58. ATGL regulation is also likely to differ between adipocytes and myocytes. Perilipin A is an integral component of the lipid droplet scaffold and is critical for ATGL-dependent lipolysis in adipocytes (30), perhaps by controlling ATGL accessibility to CGI-58 (31). In contrast,

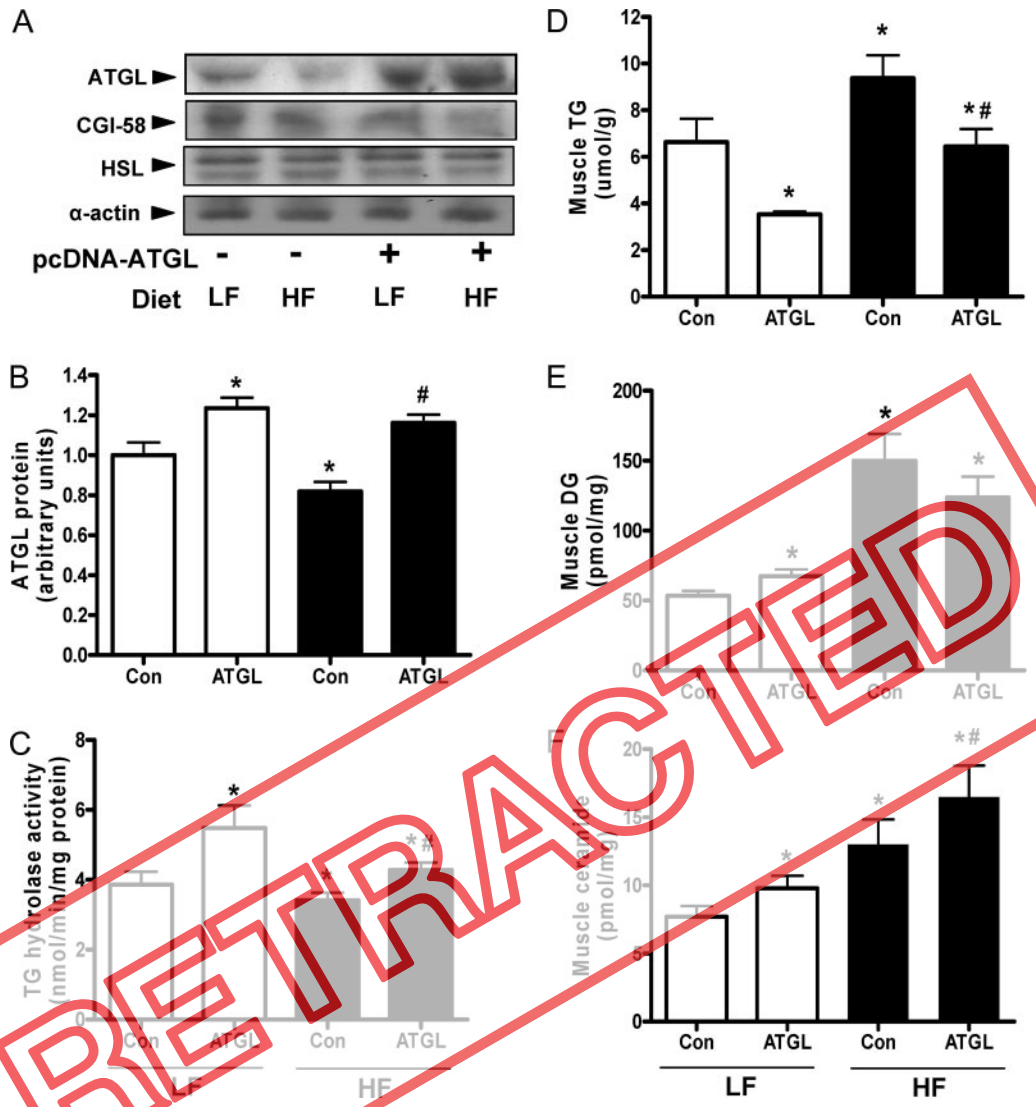

Fig. 6. ATGL Expression and Lipid Content in Skeletal Muscle of Rats with Overexpression of ATGL in the TA

A vector containing ATGL cDNA was injected into the TA of one leg and control vector (Con) into the contralateral leg. DNA was electroporated into muscles, and after 7 d recovery, ATGL, CGI-58, and HSL protein expression were determined by Western blot (A). ATGL protein expression (B), TG hydrolase activity (C; Con LF, 3.87 ± 0.36 nmol/h·mg protein), and TG (D; Con LF, 6.64 ± 0.99 μmol/g), DG (E), and ceramide (F) contents were determined in skeletal muscle lysates of rats fed either a low-fat (*white bars*) or a high-fat (*black bars*) diet. Data are mean ± SEM. *, $P < 0.05$ *vs.* control chow diet; #, $P < 0.05$ *vs.* control high-fat diet (n = 8 per group).

perilipin is not expressed in skeletal muscle but other lipid droplet-associated proteins, including adipose differentiation-related protein and tail-interacting protein of 47 kDa, are expressed and are known to regulate fat storage and lipolysis. Future imaging studies are required to address the cellular organization and interaction of lipid droplet proteins and trafficking of these proteins within skeletal muscle cells.

Concomitant with our *in vitro* studies, we have demonstrated that ATGL protein expression is reduced in the skeletal muscle of obese, insulin-resistant mice and rats. These findings are consistent with the negative regulation of ATGL by insulin in adipocytes (17, 32–34). Accordingly, we hypothesized that impaired ATGL expression may contribute to some of the metabolic defects observed in obese, insulin-resistant phenotypes and that increasing ATGL would reduce skeletal muscle lipid deposition and thereby enhance insulin's ability to stimulate glucose uptake. Stable overexpression of ATGL promoted TG lipolysis, which resulted in increased oxidation of FAs derived from TG and decreased oxidation of FA derived from the extracellular media. ATGL unexpectedly promoted the accumulation of DG, a product of the ATGL reaction, suggesting that endogenous HSL is insufficient to compensate for the increased TG turnover when ATGL activity is elevated. Ceramide levels were also increased, presumably via *de novo* synthesis from the

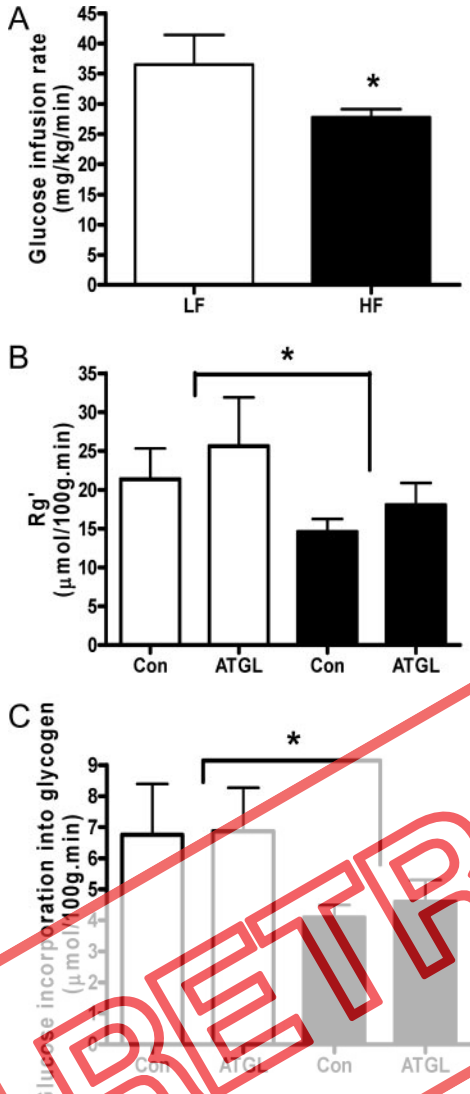

Fig. 7. Insulin Sensitivity with ATGL Overexpression *in Vivo*

Hyperinsulinemic-euglycemic clamps were conducted in Wistar rats after electroporation of a vector containing ATGL cDNA into one TA and control vector into the contralateral leg. The glucose infusion rate (A), glucose uptake into the TA (denoted as Rg', B) and glucose incorporation into glycogen within the TA (C) were determined in animals fed a chow or high-fat diet. *White bars* represent chow-fed animals, and *black bars* represent high-fat-fed animals (n = 9–10 animals per group). Data are mean ± SEM. *, $P < 0.05$ *vs.* chow diet. B and C, Main effect for high-fat diet.

Table 1. Characteristics of Rats Fed a Chow (4% Fat) or High-Fat Diet (45% fat) for Four Weeks

	Chow	High-Fat Diet
Body mass (g)	357 ± 10	367 ± 4
Epididymal fat (% body mass)	0.53 ± 0.04	1.19 ± 0.08[a]
Subcutaneous fat (% body mass)	0.94 ± 0.05	1.56 ± 0.12[a]
Plasma insulin (pmol/liter)	187 ± 22	285 ± 51[a]
Plasma glucose (mmol/liter)	7.1 ± 0.2	7.5 ± 0.1
Plasma FFA (mmol/liter)	0.48 ± 0.06	0.58 ± 0.07

[a] Different from chow ($P < 0.05$); n = 10.

excess flux of FAs within the myotube. ATGL was previously shown to possess acylglycerol transacylase activity (14), which raises the possibility that ATGL could transfer fatty acyl coenzyme A to the 1-hydroxyl position of serine to form ceramide. Interestingly, coexpression with CGI-58 amplified these effects on substrate metabolism with the exception of ceramide accumulation. Although this indicates a previously undefined role of CGI-58 in ceramide metabolism, we did not find a reduction of ceramide in myotubes overexpressing CGI-58 alone. Consistent with the scenario that DG and ceramide contribute to insulin resistance in skeletal muscle (35, 36), ATGL overexpression induced insulin resistance in ATGL-overexpressing cells as reflected in reduced insulin-stimulated glycogen synthesis.

Our fat metabolism findings from the cell culture experiments were largely replicated when ATGL was overexpressed in rats *in vivo*. Electroporation increased ATGL protein expression and TG lipase activity of chow-fed animals, resulting in DG and ceramide accumulation. When ATGL protein expression and TG hydrolase activity in the skeletal muscle of obese, insulin-resistant animals were increased to levels observed in nonobese animals, TG content was reduced and ceramide accumulated. Interestingly, muscle insulin sensitivity was not influenced by ATGL overexpression, which contrasts with the cell culture studies showing insulin resistance with ATGL overexpression. The major differences between our two approaches was that ceramides and DG accumulated in cells with ATGL overexpression (50–240%), whereas in rats, ceramides were only modestly increased irrespective of diet, and DGs were largely unaltered. The studies presented herein demonstrate that physiological increases in ATGL can alter fat metabolism that results in the accumulation of FA metabolites known to induce insulin resistance; however, small increases in ceramide and DG do not appear to reach the required threshold for induction of insulin resistance by FA metabolites. Consistent with this notion, when insulin resistance was induced using several experimental approaches, *e.g.* treating cells with palmitate (35), high-fat feeding (37), and lipid and heparin infusion in rodents/humans (35, 38–41), ceramide accumulation was more than 45% that observed in insulin-sensitive controls.

In summary, the results of the present studies provide compelling evidence that ATGL is a TG hydrolase in skeletal muscle that alters fat metabolism/partitioning both *in vitro* and *in vivo*. Although ATGL content and TG hydrolase activity are decreased in obese, insulin-resistant phenotypes, our overexpression studies indicate that this does not rescue the condition and is therefore unlikely to be a primary causal factor

of the pathogenesis of obesity-associated insulin resistance.

MATERIALS AND METHODS

Cell Culture

C2C12 myoblasts were grown in DMEM supplemented with 5 mmol/liter glucose, 10% fetal bovine serum and antibiotics. Myoblasts were grown to 80% confluence and myotube differentiation was induced by switching to medium containing 2% fetal bovine serum. Cells were used for experiments when fully differentiated, usually after 5 d. Stock FA solutions were prepared by conjugating 100 mmol/liter palmitate or 200 mmol/liter oleate, dissolved in ethanol, to 2% (wt/vol) FA-free BSA in medium with 5 mmol/liter glucose, and no antibiotics. Control medium contained 2% BSA (wt/vol) and no lipid.

siRNA Transfection in Myotubes

Gene silencing was achieved with equal efficacy using two siRNA sequences of mouse ATGL (siRNA ID 183466 and 183467; Ambion, Austin, TX) as described (42). Briefly, the cell culture medium was changed to antibiotic-free DMEM containing annealed oligonucleotides and Lipofectamine 2000 (Invitrogen, Mt. Waverley, Victoria, Australia) at d 4 of differentiation. The transfection medium was removed after 24 h, and experiments were performed. A negative control siRNA (no. 4613) was used as a partial control for off-target effects.

Construction of Expression Vectors and Generation of Cell Lines

Total RNA was isolated from mouse adipose tissue using Trizol reagent (Invitrogen) according to the manufacturer's protocol. RNA (3 μg) was reverse transcribed using the Thermoscript RT-PCR system (Invitrogen) and oligo dT primers. ATGL and CGI-58 cDNAs were PCR amplified using AmpliTaq Gold DNA polymerase (Applied Biosystems, Scoresby, Victoria, Australia) with the following primers as described (16, 18): mouse ATGL forward 5′-GGTACCGTTCCCGAGGGAGACCAAGTGGA-3′ and reverse 5′-CCTCGAGCGCAAGGCGGGAGGCCAGGT-3′ and mouse CGI-58 forward 5′-CGGATCCAAACGCGATGGCGGCGGAGGA-3′ and reverse 5′-CCTCGAGTCAGTCTACTGTGTGGCAGATCTCC-3′.

The PCR products were gel purified, subjected to restriction digestion (*Kpn*I/*Xho*I-ATGL, *Bam*HI/*Xho*I-CGI-58), subcloned into the multiple cloning site of the pcDNA/HisMax plasmid vector (Invitrogen), and sequence verified. Plasmid DNA was purified using an endotoxin-free maxiprep kit (QIAGEN, Doncaster, Victoria, Australia) for use in electroporation studies. A control pcDNA/HisMax vector was obtained from the manufacturer (Invitrogen).

C2C12 myoblasts were infected with retrovirus from Plat-E packaging cells (43) transfected with GFP- and HA-tagged ATGL (GFP-YPYDVPDYA-RSRKLRILQSTV-ATGL; GFP-HA-ATGL) or GFP-HA alone in the retroviral vector pLXIN (Clontech, Palo Alto, CA). The pLXIN/GFP-HA-ATGL construct was transfected into Plat-E cells using FuGENE, and the virus was harvested 48 h later. Virus supernatant was used to infect C2C12 myoblasts at 30% confluence. G418 selection was placed on the cells 48 h after infection. Selection was further enhanced by flow cytometric selection of fluorescent cells. Cells were used as mixed populations, and it was confirmed that all cells were fluorescent before the experiment. C2C12 myoblasts expressing GFP-HA-ATGL or GFP-HA alone were infected with retrovirus from Plat-E cells transfected with FLAG-tagged CGI-58 in the retroviral vector pBABE(puro) (44). Puromycin (2.5 mg/ml; Sigma, Castle Hill, Australia) selection was placed on the cells 48 h after infection and maintained throughout passaging. Expression was confirmed by immunoblotting.

Animal Maintenance and Surgery

Eight-week-old male C57BL/6J mice and *ob*/*ob* mice and heterozygous littermates (Monash Animal Services, Victoria, Australia) were fed either a low-fat (9% calories from fat) or high-fat (45% fat) diet for 12 wk. Animals were fasted for 4 h before experiments and were anesthetized by ip injection of sodium pentobarbital (60 mg/kg body mass). The gastrocnemius muscle was dissected and immediately frozen in liquid nitrogen. Animals were killed by lethal injection of sodium pentobarbital. For *in vivo* electroporation studies, male Wistar rats (~200 g) were fed a high-fat diet [45% fat (lard), 20% protein, 35% carbohydrates] or low-fat diet (6% fat, 21% protein, 71% carbohydrate) for 4 wk. Rats were cannulated a week before hyperinsulinemic-euglycemic clamps as described (45). Experimental procedures were approved by the St. Vincent's Hospital Animal Experimentation Ethics Committee and followed the Principles of Laboratory Animal Care.

In Vivo Electroporation

In vivo electrotransfer procedures used have been previously described (46). Anesthesia was induced, and animals' hind limbs were shaved, washed with a chlorhexidine-ethanol solution, and the TA muscles were injected in an oblique fashion transcutaneously along their length with 0.5 μg/μl total DNA. The hind limbs were electroporated, which has been shown to transfect about 50% of fibers (47). We probed for the adipocyte-specific proteins perilipin A and aP2 by Western blot and detected no signal, suggesting that there was no, or very little, contaminating adipocytes in the muscles (data not shown). Clamps were performed on animals 7 d after electrotransfer.

Hyperinsulinemic-Euglycemic Clamp and Tracer Infusion

Hyperinsulinemic-euglycemic clamping of conscious rats were performed using a previously established protocol (45), incorporating administration of a bolus injection of 2-deoxy-D-[2,6-^{3}H]glucose (Amersham Biosciences, Rydalmere, Australia). Plasma tracer disappearance was used to calculate the rate of disappearance (R_d). The glucose metabolic index (R_g') and glycogen synthesis were determined as previously described (48).

mRNA Analysis

Total RNA was extracted from tissues in 750 μl Qiazol extraction reagent followed by isolation using an RNeasy tissue kit (QIAGEN) according to the manufacturer's instructions. RNA quantity was determined at 260 nm (NanoDrop p2000 spectrometer; Biolab, Clayton, Australia). RNA was reverse transcribed (Invitrogen), and gene products were determined by real-time quantitative RT-PCR (Mx3000P; Stratagene, La Jolla, CA) using TaqMan Assays-on-Demand (Applied Biosystems). The assay ID numbers are as follows: ATGL, Mm00503040_m1; HSL, Mm00495359_m1; and 18S, Hs99999901_s1. The final reaction mix consisted of 10 μl TaqMan Universal PCR Master Mix, 100 ng cDNA in 9 μl RNase-free water, and 1 μl of supplied primers. PCR conditions were as follows: 2 min at 50 C and 10 min at 95 C, followed by 40 cycles of PCR at 95 C for 15 sec and 60 C for

45 sec. 18S was used as a reference gene and did not vary between groups. The mRNA levels were determined by a comparative cycle threshold (C_T) method. For each sample, a ΔC_T value was obtained by subtracting 18S C_T values from those of the gene of interest. The average ΔC_T value of the lean group was then subtracted from the sample to derive a $\Delta - \Delta C_T$ value. The expression of each gene was then evaluated by $2^{-(\Delta-\Delta CT)}$.

Western Blot Analysis

Cells were lysed or tissue homogenized in buffer consisting of 20 mM HEPES, 1 mM dithiothreitol, 1 mM $Na_4P_2O_7$, 2 mM EDTA, 1% Triton X-100, 10% glycerol (vol/vol), 3 mM benzamidine, 1 mM phenylmethylsulfonyl fluoride, 5 μl/ml phosphatase inhibitor cocktail 2 (Sigma), and 5 μl/ml protease inhibitor cocktail (Sigma). Solubilized whole-cell lysate proteins (30–60 μg/lane) were transferred to nitrocellulose membranes that were blocked with 5% nonfat milk. Membranes were incubated in primary antibodies (ATGL, Akt Ser473, and Akt from Cell Signaling, Danvers, MA; CGI-58 from Abnova Corp., Taipei, Taiwan). The HSL antibody was as previously described (8). Membranes were incubated with protein G Horseradish peroxidase-conjugated secondary antibody followed by immunodetection with enhanced chemiluminescence. Histochemistry images are not provided because the animal ethics committee was unlikely to extend the protocol.

Assay for TG Hydrolase Activity

TG hydrolase activity was determined in cell or tissue extracts as described (6). For adrenergic stimulation experiments, myotubes were exposed to 10 μM isoproterenol for 20 min before lysing.

Determination of FA Metabolism and Lipid Analysis

FA metabolism was performed using 0.5 μCi/ml [1-^{14}C]palmitate or 0.5 μCi/ml [1-^{14}C]oleate (Amersham Biosciences). In some experiments, myotubes were exposed to 10 μM isoproterenol for the duration of the experiment. FA pulse-chase experiments were performed to determine endogenous FA oxidation. Myotubes were pulsed with 0.25 mM [^{14}C]oleate for 24 h to prelabel intracellular lipid pools, of which 74% was incorporated into TG. The medium was replaced and FA oxidation was assessed during the chase period as described above. It is assumed that all of the oxidized oleate originated from TG. Muscle TG (49) diacylglycerol, and ceramide (50) were extracted and quantified according to published methods.

Determination of Glycogen Synthesis

Cells were pretreated for 20 h with 0.25 mmol/liter palmitate conjugated to 2% BSA or 2% BSA alone. The medium was replaced, and cells were incubated for 2 h in DMEM containing [1-^{14}C] glucose (4 μCi/ml) in the absence or presence of 100 nmol/liter insulin. Glycogen synthesis in myotubes was determined as described previously (35).

Determination of Glycogen Content

Muscle glycogen was extracted in 2 M HCl and neutralized with 0.66 M NaOH. The liberated glucosyl units were quantified by the glucose oxidase method (Sigma; GAGO-20).

Blood Treatment and Analysis

Blood was mixed in EDTA tubes and centrifuged and the plasma stored. Plasma glucose was determined using an automated glucose analyzer (YSI 2300; YSI, Yellow Springs, OH) and plasma FFA by a colorimetric method (Wako Chemicals, Richmond, VA). Basal insulin was assessed using a rat/mouse insulin ELISA (Linco, St. Charles, MO) and clamp insulin using human ELISA (Mercodia, Uppsala, Sweden).

Statistical Analysis

Statistical analysis was performed using unpaired Student's *t* test. A two-way ANOVA with repeated measures was applied where appropriate, and a Student Newman-Keuls *post hoc* analysis performed. Statistical significance was set at $P < 0.05$.

Acknowledgments

We thank Sarah Turpin for excellent technical assistance.

Received October 22, 2007. Accepted January 11, 2008.

Address all correspondence and requests for reprints to: Matthew J. Watt, Ph.D., Department of Physiology, Monash University, Clayton, Victoria, Australia 3065. E-mail: matthew.watt@med.monash.edu.au.

These studies were supported by research grants from the Australian Research Council (ARC) and the National Health and Medical Research Council of Australia (NHMRC). M.J.W. is supported by an R. Douglas Wright Fellowship, C.R.B. by a Peter Doherty Postdoctoral fellowship and E.W.K. by the NHMRC fellowship scheme. A.J.H. is supported by a University of New South Wales Postgraduate Award, and B.E.K. is an ARC Federation Fellow.

Disclosure Statement: The authors have nothing to disclose.

REFERENCES

1. Watt MJ, Heigenhauser GJ, Spriet LL 2002 Intramuscular triacylglycerol utilization in human skeletal muscle during exercise: is there a controversy? J Appl Physiol 93: 1185–1195
2. Krssak M, Falk PK, Dresner A, DiPietro L, Vogel SM, Rothman DL, Roden M, Shulman GI 1999 Intramyocellular lipid concentrations are correlated with insulin sensitivity in humans: a ^{1}H NMR spectroscopy study. Diabetologia 42:113–116
3. Pan DA, Lillioja S, Kriketos AD, Milner MR, Baur LA, Bogardus C, Jenkins AB, Storlien LH 1997 Skeletal muscle triglyceride levels are inversely related to insulin action. Diabetes 46:983–988
4. Langfort J, Ploug T, Ihlemann J, Saldo M, Holm C, Galbo H 1999 Expression of hormone-sensitive lipase and its regulation by adrenaline in skeletal muscle. Biochem J 340(Pt 2):459–465
5. Langfort J, Ploug T, Ihlemann J, Holm C, Galbo H 2000 Stimulation of hormone-sensitive lipase activity by contractions in rat skeletal muscle. Biochem J 351:207–214
6. Watt MJ, Heigenhauser GJ, Spriet LL 2003 Effects of dynamic exercise intensity on the activation of hormone-sensitive lipase in human skeletal muscle. J Physiol 547: 301–308
7. Watt MJ, Stellingwerff T, Heigenhauser GJ, Spriet LL 2003 Effects of plasma adrenaline on hormone-sensitive lipase at rest and during moderate exercise in human skeletal muscle. J Physiol 550:325–332
8. Watt MJ, Holmes AG, Pinnamaneni SK, Garnham AP, Steinberg GR, Kemp BE, Febbraio MA 2006 Regulation of HSL serine phosphorylation in skeletal muscle and adipose tissue. Am J Physiol Endocrinol Metab 290: E500–E508

9. Roepstorff C, Vistisen B, Donsmark M, Nielsen JN, Galbo H, Green KA, Hardie DG, Wojtaszewski JF, Richter EA, Kiens B 2004 Regulation of hormone-sensitive lipase activity and Ser563 and Ser565 phosphorylation in human skeletal muscle during exercise. J Physiol 560: 551–562
10. Prats C, Donsmark M, Qvortrup K, Londos C, Sztalryd C, Holm C, Galbo H, Ploug T 2006 Decrease in intramuscular lipid droplets and translocation of HSL in response to muscle contraction and epinephrine. J Lipid Res 47: 2392–2399
11. Greenberg AS, Egan JJ, Wek SA, Garty NB, Blanchette-Mackie EJ, Londos C 1991 Perilipin, a major hormonally regulated adipocyte-specific phosphoprotein associated with the periphery of lipid storage droplets. J Biol Chem 266:11341–11346
12. Haemmerle G, Zimmermann R, Hayn M, Theussl C, Waeg G, Wagner E, Sattler W, Magin TM, Wagner EF, Zechner R 2002 Hormone-sensitive lipase deficiency in mice causes diglyceride accumulation in adipose tissue, muscle, and testis. J Biol Chem 277:4806–4815
13. Watt MJ, Steinberg GR, Chan S, Garnham A, Kemp BE, Febbraio MA 2004 β-Adrenergic stimulation of skeletal muscle HSL can be overridden by AMPK signaling. FASEB J 18:1445–1446
14. Jenkins CM, Mancuso DJ, Yan W, Sims HF, Gibson B, Gross RW 2004 Identification, cloning, expression, and purification of three novel human calcium-independent phospholipase A2 family members possessing triacylglycerol lipase and acylglycerol transacylase activities. J Biol Chem 279:48968–48975
15. Villena JA, Roy S, Sarkadi-Nagy E, Kim KH, Sul HS 2004 Desnutrin, an adipocyte gene encoding a novel patatin domain-containing protein, is induced by fasting and glucocorticoids: ectopic expression of desnutrin increases triglyceride hydrolysis. J Biol Chem 279: 47066–47075
16. Zimmermann R, Strauss JG, Haemmerle G, Schoiswohl G, Birner-Gruenberger R, Riederer M, Lass A, Neuberger G, Eisenhaber F, Hermetter A, Zechner R 2004 Fat mobilization in adipose tissue is promoted by adipose triglyceride lipase. Science 306:1383–1386
17. Kershaw EE, Hamm JK, Verhagen LA, Peroni O, Katic M, Flier JS 2006 Adipose triglyceride lipase: function, regulation by insulin, and comparison with adiponutrin. Diabetes 55:148–157
18. Lass A, Zimmermann R, Haemmerle G, Riederer M, Schoiswohl G, Schweiger M, Kienesberger P, Strauss JG, Gorkiewicz G, Zechner R 2006 Adipose triglyceride lipase-mediated lipolysis of cellular fat stores is activated by CGI-58 and defective in Chanarin-Dorfman syndrome. Cell Metab 3:309–319
19. Gronke S, Mildner A, Fellert S, Tennagels N, Petry S, Muller G, Jackle H, Kuhnlein RP 2005 Brummer lipase is an evolutionary conserved fat storage regulator in *Drosophila*. Cell Metab 1:323–330
20. Haemmerle G, Lass A, Zimmermann R, Gorkiewicz G, Meyer C, Rozman J, Heldmaier G, Maier R, Theussl C, Eder S, Kratky D, Wagner EF, Klingenspor M, Hoefler G, Zechner R 2006 Defective lipolysis and altered energy metabolism in mice lacking adipose triglyceride lipase. Science 312:734–737
21. Savage DB, Petersen KF, Shulman GI 2007 Disordered lipid metabolism and the pathogenesis of insulin resistance. Physiol Rev 87:507–520
22. Baron AD, Brechtel G, Wallace P, Edelman SV 1988 Rates and tissue sites of non-insulin- and insulin-mediated glucose uptake in humans. Am J Physiol 255: E769–E774
23. Zurlo F, Larson K, Bogardus C, Ravussin E 1990 Skeletal muscle metabolism is a major determinant of resting energy expenditure. J Clin Invest 86:1423–1427
24. Steinberg GR, Kemp BE, Watt MJ 2007 Adipocyte triglyceride lipase expression in human obesity. Am J Physiol Endocrinol Metab 293:E958–E964
25. Bastie CC, Hajri T, Drover VA, Grimaldi PA, Abumrad NA 2004 CD36 in myocytes channels fatty acids to a lipase-accessible triglyceride pool that is related to cell lipid and insulin responsiveness. Diabetes 53:2209–2216
26. Chanarin I, Patel A, Slavin G, Wills EJ, Andrews TM, Stewart G 1975 Neutral-lipid storage disease: a new disorder of lipid metabolism. Br Med J 1:553–555
27. Turpin SM, Lancaster GI, Darby I, Febbraio MA, Watt MJ 2006 Apoptosis in skeletal muscle myotubes is induced by ceramides and is positively related to insulin resistance. Am J Physiol Endocrinol Metab 291:E1341–E1350
28. Lake AC, Sun Y, Li JL, Kim JE, Johnson JW, Li D, Revett T, Shih HH, Liu W, Paulsen JE, Gimeno RE 2005 Expression, regulation, and triglyceride hydrolase activity of Adiponutrin family members. J Lipid Res 46:2477–2487
29. Smirnova E, Goldberg EB, Makarova KS, Lin L, Brown WJ, Jackson CL 2006 ATGL has a key role in lipid droplet/adiposome degradation in mammalian cells. EMBO Rep 7:106–113
30. Miyoshi H, Perfield 3rd JW, Souza SC, Shen WJ, Zhang HH, Stancheva ZS, Kraemer FB, Obin MS, Greenberg AS 2006 Control of adipose triglyceride lipase action by serine 517 of perilipin A globally regulates protein kinase A-stimulated lipolysis in adipocytes. J Biol Chem 282: 996–1002
31. Granneman JG, Moore HP, Granneman RL, Greenberg AS, Obin MS, Zhu Z 2007 Analysis of lipolytic protein trafficking and interactions in adipocytes. J Biol Chem 282:5726–5735
32. Kim JY, Tillison K, Lee JH, Rearick DA, Smas CM 2006 The adipose tissue triglyceride lipase ATGL/PNPLA2 is downregulated by insulin and TNF-α in 3T3-L1 adipocytes and is a target for transactivation by PPARγ. Am J Physiol Endocrinol Metab 291:E115–E127
33. Kralisch S, Klein J, Lossner U, Bluher M, Paschke R, Stumvoll M, Fasshauer M 2005 Isoproterenol, TNFα, and insulin downregulate adipose triglyceride lipase in 3T3–L1 adipocytes. Mol Cell Endocrinol 240:43–49
34. Jocken JW, Langin D, Smit E, Saris WH, Valle C, Hul GB, Holm C, Arner P, Blaak EE 2007 Adipose Triglyceride lipase and hormone-sensitive lipase protein expression is decreased in the obese insulin-resistant state. J Clin Endocrinol Metab 92:2292–2299
35. Schmitz-Peiffer C, Craig DL, Biden TJ 1999 Ceramide generation is sufficient to account for the inhibition of the insulin-stimulated PKB pathway in C2C12 skeletal muscle cells pretreated with palmitate. J Biol Chem 274: 24202–24210
36. Yu C, Chen Y, Cline GW, Zhang D, Zong H, Wang Y, Bergeron R, Kim JK, Cushman SW, Cooney GJ, Atcheson B, White MF, Kraegen EW, Shulman GI 2002 Mechanism by which fatty acids inhibit insulin activation of insulin receptor substrate-1 (IRS-1)-associated phosphatidylinositol 3-kinase activity in muscle. J Biol Chem 277:50230–50236
37. Watt MJ, Dzamko N, Thomas WG, Rose-John S, Ernst M, Carling D, Kemp BE, Febbraio MA, Steinberg GR 2006 CNTF reverses obesity-induced insulin resistance by activating skeletal muscle AMPK. Nat Med 12: 541–548
38. Holland WL, Brozinick JT, Wang LP, Hawkins ED, Sargent KM, Liu Y, Narra K, Hoehn KL, Knotts TA, Siesky A, Nelson DH, Karathanasis SK, Fontenot GK, Birnbaum MJ, Summers SA 2007 Inhibition of ceramide synthesis ameliorates glucocorticoid-, saturated-fat-, and obesity-induced insulin resistance. Cell Metab 5:167–179
39. Watt MJ, Hevener A, Lancaster GI, Febbraio MA 2006 Ciliary neurotrophic factor prevents acute lipid-induced insulin resistance by attenuating ceramide accumulation

and phosphorylation of c-Jun N-terminal kinase in peripheral tissues. Endocrinology 147:2077–2085
40. Adams 2nd JM, Pratipanawatr T, Berria R, Wang E, DeFronzo RA, Sullards MC, Mandarino LJ 2004 Ceramide content is increased in skeletal muscle from obese insulin-resistant humans. Diabetes 53:25–31
41. Straczkowski M, Kowalska I, Nikolajuk A, Dzienis-Straczkowska S, Kinalska I, Baranowski M, Zendzian-Piotrowska M, Brzezinska Z, Gorski J 2004 Relationship between insulin sensitivity and sphingomyelin signaling pathway in human skeletal muscle. Diabetes 53: 1215–1221
42. Pinnamaneni SK, Southgate RJ, Febbraio MA, Watt MJ 2006 Stearoyl CoA desaturase 1 is elevated in obesity but protects against fatty acid-induced skeletal muscle insulin resistance in vitro. Diabetologia 49:3027–3037
43. Morita S, Kojima T, Kitamura T 2000 Plat-E: an efficient and stable system for transient packaging of retroviruses. Gene Ther 7:1063–1066
44. Morgenstern JP, Land H 1990 Advanced mammalian gene transfer: high titre retroviral vectors with multiple drug selection markers and a complementary helper-free packaging cell line. Nucleic Acids Res 18:3587–3596
45. Clark PW, Jenkins AB, Kraegen EW 1990 Pentobarbital reduces basal liver glucose output and its insulin suppression in rats. Am J Physiol 258:E701–E707
46. Bruce CR, Brolin C, Turner N, Cleasby ME, van der Leij FR, Cooney GJ, Kraegen EW 2007 Overexpression of carnitine palmitoyltransferase I in skeletal muscle in vivo increases fatty acid oxidation and reduces triacylglycerol esterification. Am J Physiol Endocrinol Metab 292: E1231–E1237
47. Cleasby ME, Davey JR, Reinten TA, Graham MW, James DE, Kraegen EW, Cooney GJ 2005 Acute bidirectional manipulation of muscle glucose uptake by in vivo electrotransfer of constructs targeting glucose transporter genes. Diabetes 54:2702–2711
48. James DE, Kraegen EW, Chisholm DJ 1985 Effects of exercise training on in vivo insulin action in individual tissues of the rat. J Clin Invest 76:657–666
49. Bergmeyer HU 1974 Methods in enzymatic analysis. New York: Academic
50. Preiss J, Loomis CR, Bishop WR, Stein R, Niedel JE, Bell RM 1986 Quantitative measurement of sn-1,2-diacylglycerols present in platelets, hepatocytes, and ras- and sis-transformed normal rat kidney cells. J Biol Chem 261:8597–8600

Molecular Endocrinology **is published monthly by The Endocrine Society (http://www.endo-society.org), the foremost professional society serving the endocrine community.**